Angewandte Chemie
Eine Zeitschrift der Gesellschaft Deutscher Chemiker

Supporting Information

# Mapping Hydration Water around Alcohol Chains by THz Calorimetry

*Fabian Böhm, Gerhard Schwaab, and Martina Havenith**

anie_201612162_sm_miscellaneous_information.pdf

**Supplementary information:**

We recorded temperature-dependent, low frequency spectra of five alcohols with variable hydrocarbon chain length (methanol, ethanol, propanol, butanol, pentanol) and a branched alcohol (tert-butanol). Spectra of sample solutions with concentrations of 0.5M (0.2M for PeOH) were recorded at five different temperatures (0°C, 10°C, 20°C, 30°C, and 40°C) in the frequency range between 50 and 350 $cm^{-1}$ using FTIR absorption spectrometer.

We used a Bruker Vertex 80v FTIR spectrometer equipped with a liquid helium cooled silicon bolometer from Infrared Laboratories as a detector. The sample solutions were placed in a temperature controlled liquid transmission cell from Harrick with two amorphous diamond windows of 0.5 mm thickness supplied by Diamond Materials and a Kapton spacer of ca. 30 µm thickness. The sample layer thickness was determined by recording etalons of the empty cell prior to each measurement. For each single spectrum, 64 scans were averaged with a frequency resolution of 2 $cm^{-1}$. During each series of measurements, the sample compartment was constantly purged with technical grade dry nitrogen to minimize humidity. Using Lambert-Beer's Law, the frequency and temperature dependent absorption coefficient $\alpha(\nu, T)$ is expressed as:

$$\alpha_{solution}(\tilde{\nu}, T) = \frac{1}{d} log\left(\frac{I_{water}(\tilde{\nu}, T)}{I_{solution}(\tilde{\nu}, T)}\right) + \alpha_{water}(\tilde{\nu}, T)\,,$$

where $d$ is the sample thickness, $I_{water}(\tilde{\nu}, T)$ and $I_{solution}(\tilde{\nu}, T)$ are the transmitted intensities of the water reference and the sample at temperature $T$, respectively. $\alpha_{water}(\tilde{\nu}, T)$ was deduced from a fit of the absorption spectrum of water at a given temperature $T$.[1],[2] Water was taken as a reference. This helped to eliminate spectral features due to reflections at the cell windows of the sample cell. The remaining absorption due to residual air in the absorption path was corrected by taking into account a scaled spectrum of water vapor.

The effective absorption of the solvated solute can be deduced from the following equation:

$$\alpha^{eff}_{solute}(\tilde{\nu}, T) = \alpha_{solution}(\tilde{\nu}, T) - \frac{c_\omega}{c^0_\omega}\alpha_{water}(\tilde{\nu}, T), \qquad (1)$$

where $c_\omega$ and $c^0_\omega$ are the actual water concentrations in the solution and in bulk water, respectively.

The effective molar extinction of the solute is:

$$\varepsilon^{eff}_{solute}(\tilde{\nu}, T) = \frac{\alpha^{eff}_{solute}(\tilde{\nu}, T)}{c_s} \qquad (2)$$

The result for $\varepsilon^{eff}_{solute}(\tilde{\nu}, T)$ for each alcohol solution is shown in Figure S1.

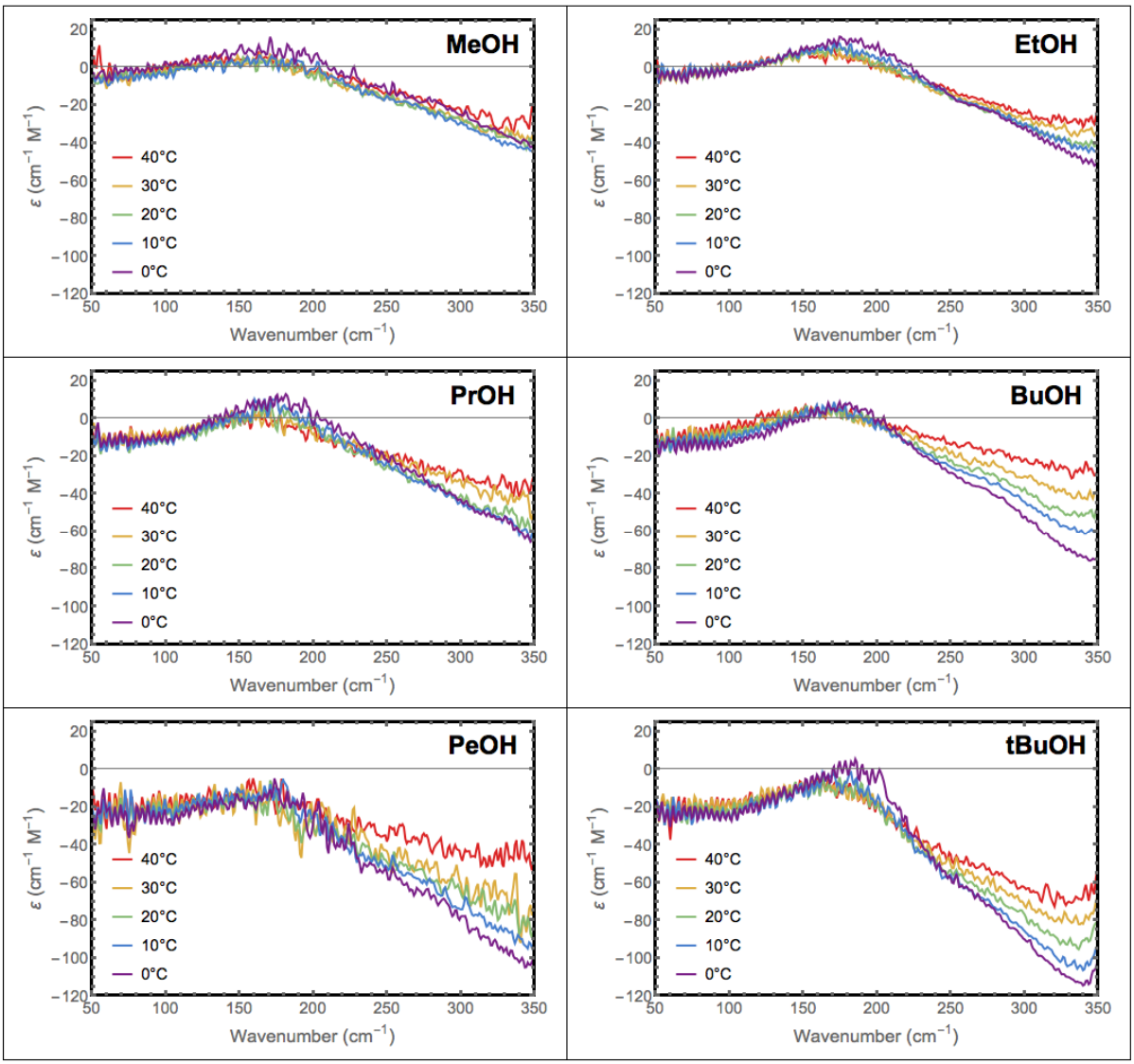


**Figure S1:** Effective molar extinction spectra for the six investigated alcohols after subtraction of the bulk water partial spectrum as a function of temperature.

The experimental molar extinction spectra are dissected into three contributions:

$$\alpha_{solute}^{eff} = \alpha_s + \alpha_{w,b} + \alpha_{w,h} = c_s\varepsilon_s + c_{w,b}\varepsilon_{w,b} + c_{w,h}\varepsilon_{w,h} \qquad (3)$$

where $\alpha_{solute}, \alpha_{w,b}$ and $\alpha_{w,h}$ are the effective absorption coefficients of the solute, bulk water and hydration water, respectively. Effective in this respect means that absorption coefficients are ensemble averages that are referenced to bulk water absorption and the solute concentration (see equation 1,2,3). $c_s, \varepsilon_s, c_{w,b}, \varepsilon_{w,b}, c_{w,h}$ and $\varepsilon_{w,h}$ are the solute concentration, the effective molar solute extinction, the bulk water concentration, the effective molar bulk water absorption, the concentration of hydration water, the effective molar absorption of hydration water, respectively.

Inserting equation (1) into equation (3) we obtain:

$$\alpha_{solute}^{eff} = \alpha_{solution} - \frac{c_w}{c_w^0}\alpha_{w,b} = c_s\varepsilon_s + c_{w,b}\varepsilon_{w,b} + c_{w,h}\varepsilon_{w,h} - \left(c_{w,h} + c_{w,b}\right)\varepsilon_{w,b}$$

$$\alpha_{solute}^{eff} = c_s\varepsilon_s + c_{w,h}(\varepsilon_{w,h} - \varepsilon_{w,b}) \qquad (4)$$

The effective molar solute extinction can be described as:

$$\varepsilon_{solute}^{eff} = \varepsilon_s + n_{w,h}\varepsilon_{w,h} - n_{w,h}\varepsilon_{w,b} \qquad (5)$$

with $n_{w,h} = c_{w,h}/c_s$ being the effective number of hydration water molecules per solute molecule. $n_{w,h}$ is increasing with increasing chain length or decreasing temperature.

This means that the effective solute extinction can be described as a (positive) contribution due to the absorption of the solute and hydration water, and a (negative) contribution taking into account the water molecules that differ in their spectral properties from the bulk water spectrum. $n_{w,h}$ provides a lower limit of effected water molecules per solute, since only water molecules which exhibit large spectral changes compared to bulk water are taking into account.

The experimental molar extinction spectra was fitted using a superposition of a negative contribution describing the lack of bulk water ($-n_{w,h}\varepsilon_{w,b}$) and a positive contribution for the hydration water described by a sum of damped harmonic oscillator functions:

$$\varepsilon_{DH}(\tilde{\nu}) = \frac{a\cdot\omega^2\cdot\tilde{\nu}^2}{4\pi^3\left((\tilde{\nu}_d^2+\frac{\omega^2}{4\pi^2}-\tilde{\nu}^2)^2+\frac{\omega^2}{\pi^2}\tilde{\nu}^2\right)}\ , \qquad (6)$$

with $a$, $w$, and $\nu_d$ describing the amplitude, the width and the center frequency of the mode. The unperturbed center frequency can then be deduced accordingly:

$$\nu_0 = \sqrt{\tilde{\nu}_d^2 + (\frac{\omega}{2\pi})^2} \qquad (7)$$

The spectrum of bulk water spectrum has been published before [3]. In Fig. S2 we show the spectrum of bulk water and ice. The frozen water layer shows two narrow peaks at 158 and at 214 $cm^{-1}$. For a clathrate (19% THF, 0°C) we observed also two hydration water bands at $\nu_1$ = 161 $cm^{-1}$ and $\nu_2$ = 203 $cm^{-1}$.

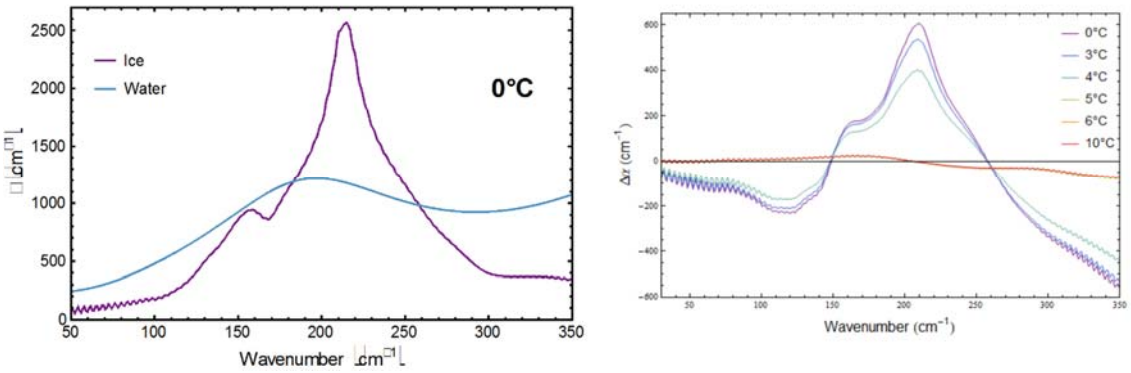


Fig. S2: Spectrum of bulk water and ice (left) and spectrum of the clathrate THF (19%) at different temperatures. Clearly, the same two red and blue shifted features are present in the spectrum.

Interestingly, we find, that the main contribution of hydration water for *all* solvated alcohols between 0°C and 40 °C, can be decomposed into *two* bands with unperturbed center frequencies of 164 $cm^{-1}$ and 195 $cm^{-1}$. This decomposition resembles the spectral features of ice and clathrates. While the amplitude of each of these two bands $\nu_{164}$ and $\nu_{195}$ is temperature and solute dependent, the center frequency and the line width is kept constant in the final global fit irrespective of the choice of solute and temperature.

In some cases (MeOH, EtOH, BuOH, tBuOH) a scaled low frequency part of the bulk water spectrum had to be added to the fit to optimize the representation of the low frequency part of the observed spectra. For butanol an additional weak band at a frequency of 270 $cm^{-1}$ was observed and included in the fit. Intramolecular bands of ethanol, butanol, pentanol and tert-butanol will fall outside of our scan range (50-350 $cm^{-1}$). These features were taken into account by adding a band with a center frequency fixed to 360 $cm^{-1}$.

We assume that the number of water molecules contributing to the hydration bands at 164 $cm^{-1}$ and 195 $cm^{-1}$ is proportional to the amplitudes at the peak center, respectively. A boundary condition is that the sum of $n_{164}$ and $n_{195}$ must be equal to $n_{w,h}$, i.e. the total number of affected water molecules per solute. This yields

$$n_\nu = \frac{a_\nu n_{w,h}}{a_{164}+a_{195}} \qquad (8)$$

with $\nu$ = 164 or 195 $cm^{-1}$. The corresponding values and their statistical 2 σ errors are given in Table S1.

**Table S1:** Number of affected water molecules in the hydration water bands $\nu_{164}$ and $\nu_{195}$ determined from the THz spectra.

| | | MeOH | EtOH | PrOH | BuOH | PeOH | tBuOH |
|---|---|---|---|---|---|---|---|
| $n_{164}$ | 0°C | 1.48(6) | 1.58(7) | 1.90(9) | 2.67(17) | 3.22(13) | 3.59(17) |
| | 10°C | 1.51(6) | 1.54(7) | 1.96(8) | 2.49(14) | 3.15(12) | 3.61(15) |
| | 20°C | 1.50(6) | 1.53(6) | 1.80(7) | 2.24(12) | 2.82(10) | 3.44(13) |
| | 30°C | 1.46(6) | 1.39(6) | 1.64(7) | 1.68(8) | 2.40(9) | 3.19(11) |
| | 40°C | 1.18(6) | 1.21(6) | 1.40(6) | 1.30(7) | 1.68(7) | 2.79(11) |
| $n_{195}$ | 0°C | 1.34(6) | 2.11(7) | 2.55(9) | 3.53(19) | 3.90(13) | 5.61(17) |
| | 10°C | 1.20(6) | 1.38(6) | 1.86(8) | 2.11(13) | 2.51(11) | 3.91(15) |
| | 20°C | 0.71(6) | 1.05(6) | 1.37(7) | 1.36(10) | 1.57(11) | 2.61(13) |
| | 30°C | 0.46(6) | 0.65(6) | 0.61(7) | 0.69(7) | 1.24(9) | 1.66(12) |
| | 40°C | 0.26(5) | 0.44(5) | 0.35(6) | 0.34(6) | 0.85(7) | 1.0(10) |

The temperature dependence of $n_{164}$ and $n_{195}$ can be well approximated by a two-state model [3]

$$n_\nu(T) = \frac{n_\nu(0)}{1+e^{\frac{\Delta H_\nu}{R}\left(\frac{1}{T}-\frac{1}{T_{\nu,\,\mathrm{melt}}}\right)}} \qquad (9)$$

with $\Delta H_\nu$ being the enthalpic energy difference between the involved states, R the universal gas constant. $T_{\nu,\,\mathrm{melt}}$, the melting temperature, being the temperature where both states are equally populated. Here we also refer to the paper of Dor Ben Amotz. [6] The results of a fit are summarized in Table S2.

**Table S2:** Results of a global two component fit of the observed hydration numbers as a function of temperature. MeOH or EtOH means that this parameter was fixed to the same parameter as for methanol and ethanol, respectively.

| | Methanol | Ethanol | Propanol | Butanol | Pentanol | Tert-BuOH |
|---|---|---|---|---|---|---|
| $n_{164}(0)$ | 1.56(7) | 1.58(7) | 1.96(8) | 2.74(13) | 3.34(12) | 3.65(9) |
| $\Delta H_{164}$ in kJ/mol | 63(10) | MeOH | MeOH | MeOH | MeOH | MeOH |
| $T_{164,\,\mathrm{ref}}$ in K | 330(5) | MeOH | 325(5) | 311(2) | 314(2) | 329(4) |
| $n_{195}(0)$ | 3.1(6) | 4.7(10) | 5.7(12) | 7.2(15) | 8.4(17) | 12.4(26) |
| $\Delta H_{195}$ in kJ/mol | 35(5) | 40(3) | EtOH | EtOH | EtOH | EtOH |
| $T_{195,\,\mathrm{melt}}$ in K | 271(6) | MeOH | MeOH | MeOH | MeOH | MeOH |

The optimum fit in respect of a minimum number of fitting parameters (Ockham's razor) and minimum $\chi^2$ was obtained assuming identical $\Delta H_{164}$, and identical $\Delta H_{195}$ and $T_{195,melt}$ for all alcohols (with the exception of MeOH). Within experimental uncertainty, $T_{164,\,\mathrm{ref}}$ for MeOH and EtOH was the same. The comparison between the results of the fit (line) and experimental data (dots) are shown in Figures S3 and S4.

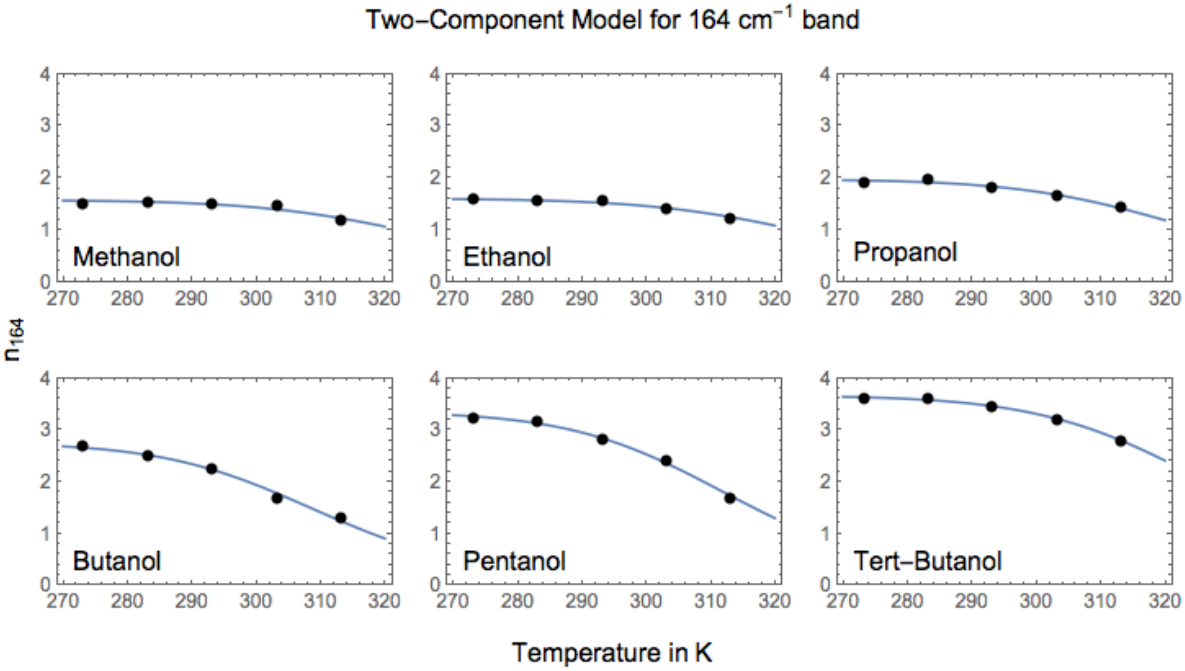


**Figure S3:** Two component model fit (line) and experimental data (points) for the 164 cm$^{-1}$ band and different alcohols.

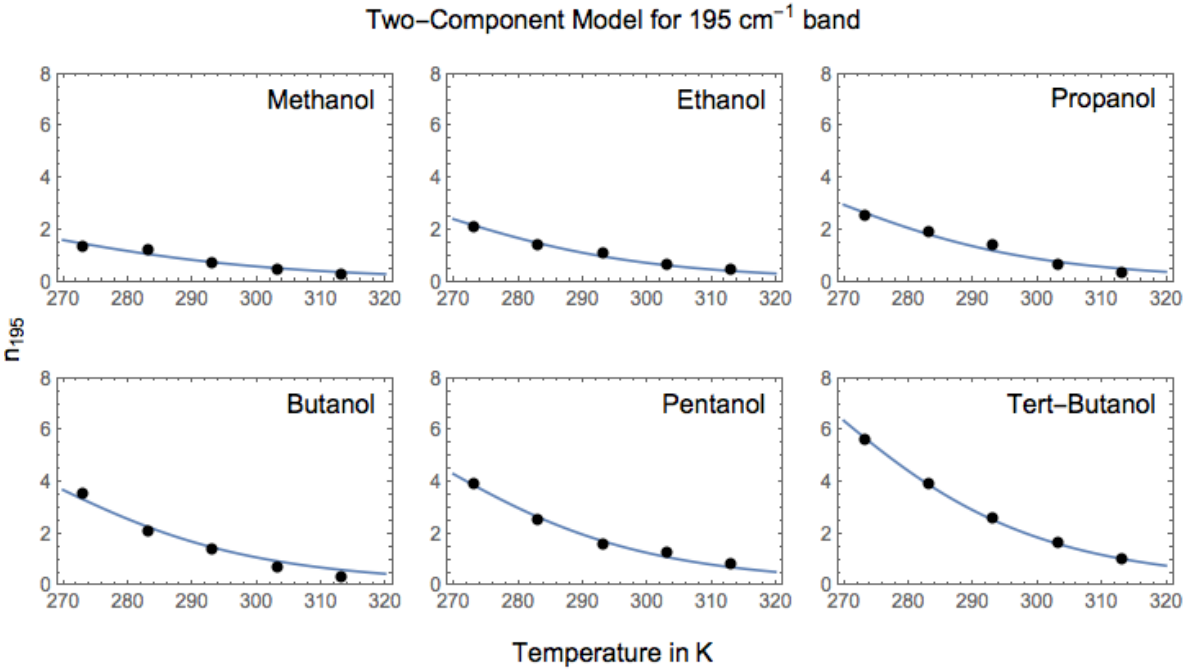


**Figure S4:** Two component model fit (line) and experimental data (points) for the 195 $cm^{-1}$ band and different alcohols.

In the following we decompose the hydration water spectra into a sum of the contribution of each individual methyl ($-CH_3$), methylene ($-CH_2-$), and hydroxyl (-OH) groups. For simplification we assume that the central carbon atom of tBuOH does not contribute due to a lack of contact with water. All other groups were weighted equally, independent of their position: *a* describes the partial amplitude of the specific hydration water band:

$$a_{i,CH_2} = \frac{a_{i,PeOH} - a_{i,MeOH}}{4}$$

$$a_{i,CH_3} = \frac{4a_{i,tBuOH} - (a_{i,BuOH} + a_{i,PrOH} + a_{i,EtOH} + a_{i,MeOH} + 6a_{i,CH_2})}{8}$$

$$a_{i,OH} = \frac{a_{i,tBuOH} + a_{i,PeOH} + a_{i,BuOH} + a_{i,PrOH} + a_{i,EtOH} + a_{i,MeOH} - 8a_{i,CH_3} - 10a_{i,CH_2}}{6} \qquad (10)$$

The result is shown in Figure S5

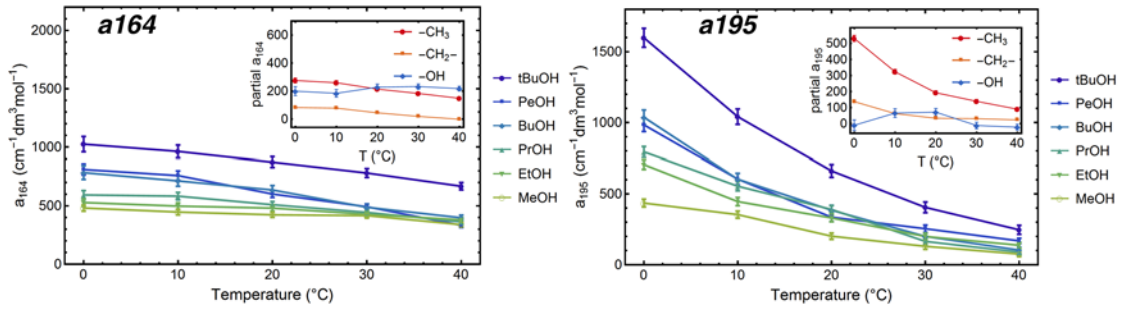


Figure S5: Temperature dependence of the amplitudes of the two modes hydration water $\nu_{164}$ and $\nu_{195}$ for each alcohol. Plotted is "a" the partial amplitude of the specific hydration water band (see SI for details). Inset: Plotted is the partial contribution of each functional group.

Now we introduce the experimental counterpart to the theoretical concept of water mapping [5]. Each partial hydration water mode contribution probes a distinct water network structure with a specific contribution to heat capacity, enthalpy, entropy and free energy. Thus, $\nu_{164}$ and $\nu_{195}$ are each assigned a mode specific heat capacity $C_p$, which differs from bulk water, i.e. $C_p^{164}$ and $C_p^{195}$. The partial contribution of each of these modes to the hydration water is described by $n_{164}(T)$ und $n_{195}(T)$. The mixing heat capacity $\Delta C_p$ is defined as the difference between $C_p$ of the mixture and the sum of the individual contributions of the two components, scaled by the solute concentration:

$$\Delta C_p(T) = \frac{1}{c_{alc}}\left(C_{p_{mixture}}(T) - \left(c_{w,tot}\, C_{p_{w,bulk}}(T) + c_{alc}\, C_{p_{alc,liquid}}(T)\right)\right) \quad (11)$$

,where $c_{w,tot}$ is the total water concentration of the sample and $C_{p_{alc,liquid}}$ is the molar heat capacity $C_p$ of alcohol in the liquid phase.

Based upon $C_p(T)$ the temperature dependence of the mixing entropy $S$, enthalpy $H$ can be determined:
$S(T_1) = S(T_0) + \int_{T_0}^{T_1} \frac{C_{p(T)}}{T} dT$ and $H(T_1) = H(T_0) + \int_{T_0}^{T_1} C_p(T)\, dT$. (12)

We now make the following ansatz for the mixing heat capacity:

$$\Delta C_p(T) = n_{164}(T)\left(C_p^{164} - C_p^{w,bulk}\right) + n_{195}(T)\left(C_p^{195} - C_p^{w,bulk}\right) + c_{alc}\ \Delta C_p^{solute} \quad (13)$$

The temperature dependence of $\Delta C_p$ is then exclusively due to changes in $n_{164}(T)$ and $n_{195}(T)$, while $\left(C_p^{164} - C_p^{w,bulk}\right) = \Delta C_p^{164}$ and $\left(C_p^{195} - C_p^{w,bulk}\right) = \Delta C_p^{195}$ and $\Delta C_p^{solute}$ are temperature independent. $\Delta C_p^{solute}$ is a solute-specific parameter which summarizes all solute-specific changes of the heat capacity at a given reference temperature. $n_{164}(T)$ and $n_{195}(T)$ in the temperature range between 0°C and 40°C is deduced from the THz measurements. In the following, $\Delta C_p^{164}$, $\Delta C_p^{195}$ as well as the constant offset at a given reference temperature (25°C) for each solute and each quantity were fitted to reproduce the temperature dependent literature values $\Delta C_p$(T), $\Delta S(T)$, and $\Delta H$(T) ) [1],[2]. In total, 20 parameters (including 18 offsets) were fitted to reproduce the macroscopic calorimetric observables $\Delta C_p(T)$, $\Delta S(T)$, and $\Delta H(T)$ for all temperatures and all alcohol chains (120 data points. The fitted parameters are summarized in Table S3:

**Table S3:** Results of a simultaneous fit of all alcohol solutions using $n_{164}(T)$ and $n_{195}(T)$ as input. Values are given in J/mol/K for $C_p$ and $\Delta S^0$; $\Delta H^0$ is given in kJ/mol. The reference temperature is 25°C. $\Delta C_p^{164}$, $\Delta C_p^{195}$ are the difference in heat capacity compared to bulk water. $C_p^0$, $S^0$, and $H^0$ are values at a reference temperature of 25°C.

| | Hydration | MeOH | EtOH | PrOH | BuOH | PeOH | tBuOH |
|---|---|---|---|---|---|---|---|
| $\Delta C_p^{164}$ | 35(3) | | | | | | |
| $\Delta C_p^{195}$ | 8.4(9) | | | | | | |
| $\Delta C_p^0$ | | 20(3) | 93(3) | 145(4) | 185(5) | 224(6) | 113(7) |
| $\Delta S^0$ | | -28.52(3) | -45.41(3) | -56.21(3) | -63.76(4) | -70.38(4) | -79.23(3) |
| $-\Delta H^0$ | | 7.273(7) | 10.160(7) | 10.183(7) | 9.248(10) | 7.910(9) | 17.392(8) |

Fig. S6 shows the remarkable quantitative agreement between the predicted temperature changes and the literature values! The blue line corresponds to the well-known *macroscopic calorimetric* values, the red dots are the predicted values based solely on the *spectroscopic* observables, $n_{164}$ and $n_{195}$, probing the *local* hydration. Note that *only two* parameters, $\Delta C_p^{164}$ and $\Delta C_p^{195}$, are sufficient to describe the temperature dependence of *all* alcohols. Based on our result any specific temperature-dependent change in $\Delta C_p$ can be explained by the change in the hydration water localized around the $CH_3$ and the OH moieties.

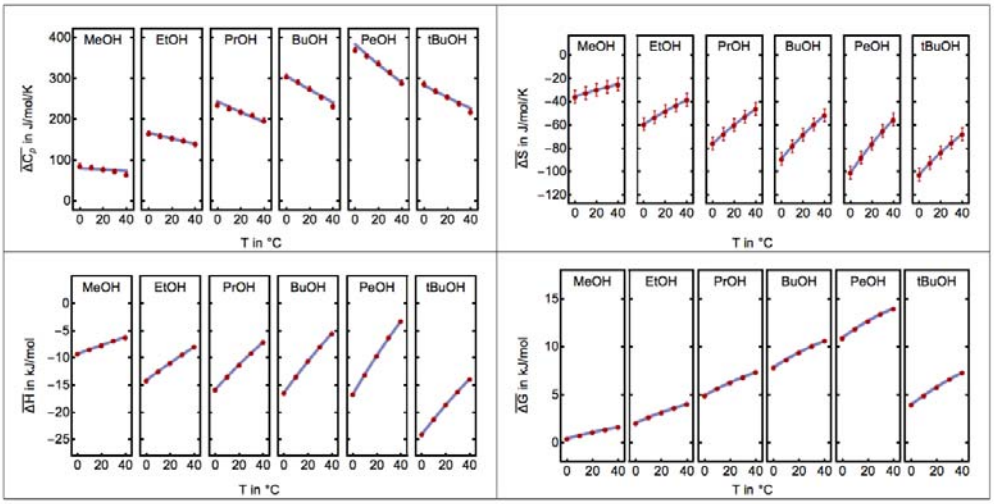


Figure S6 THz-calorimetry probing hydrophobic hydration: Displayed are the tabulated temperature and solute-dependent changes in heat capacity, entropy, enthalpy and free energy taken from previous calorimetric references [2],[3] (blue line) and the values deduced by THz-calorimetry (red dots) where the temperature and solute dependent low frequency spectra serve as an input.

In a next step we aimed to separate the temperature dependence of the thermodynamic functions related to the observed spectral changes that are correlated to local hydration changes from the global solvation changes. We used a reference temperature of 400 K well beyond the largest melting temperature of 330 K for the 164 $cm^{-1}$ band and calculated any change in thermodynamic parameter with respect to this reference temperature. Due to the lack of analytic expressions for the integrals needed to calculate $\Delta H$ and $\Delta S$, we interpolated the two-state model curves with an interpolation point spacing of 1 K and used numerical integration of the corresponding interpolated functions between 400 K and the target temperature. $\Delta G = \Delta H - T\Delta S$ was calculated from the functions obtained for $\Delta H$ and $\Delta S$. Since the value ranges of ($\Delta C_p$, $\Delta S$) and ($\Delta H$, $\Delta G$) differ by one to two orders of magnitude, different statistical weights were used in the final global fit. The weights were estimated from the approximate uncertainty in the literature thermodynamic data and were set to 0.04, 2500, 0.01, and 0.25 for $\Delta C_p$, $\Delta S$, $\Delta H$, and $\Delta G$, respectively. The large weight of $\Delta S$ only reflects the fact that $\Delta S = (\Delta H - \Delta G)/T$ and therefore the effective errors in $\Delta S$ are smaller due to the division by $T \approx 300$ K. The results of the fit at 400 K are shown in Table S4 and displayed in Figure S5. If we carry out a new fit using the calorimetric data at 400 K as reference, we obtain - within the error bars - the same values for $\Delta C_p^{164}, \Delta C_p^{195}$, and $C_p^0$, only the offset (now extrapolated to 400 K) changes (see Tab. S4).

**Table S4:** Results of a simultaneous fit of all alcohol solutions using $n_{164}(T)$ and $n_{195}(T)$ as inputs. Values are given in J/mol/K for $C_p$ and $\Delta S^0$; $\Delta H^0$ is given in kJ/mol. $C_p^0$, $S^0$, and $H^0$ are values at a reference temperature of 400 K.

| | Hydration | MeOH | EtOH | PrOH | BuOH | PeOH | tBuOH |
|---|---|---|---|---|---|---|---|
| $\Delta C_p^{164}$ | 35.5(2.3) | | | | | | |
| $\Delta C_p^{195}$ | 8.2(8) | | | | | | |
| $\Delta C_p 400$ | | 19(3) | 93(3) | 145(3) | 184(4) | 223(5) | 111(6) |
| $\Delta S 400$ | | -16.6(5) | -11.9(5) | -6.7(6) | -3.8(9) | +3.3(1.0) | -32(1.0) |
| $\Delta H 400$ | | -3.3(0.2) | 1.3(0.2) | 6.8(0.2) | 11.4(0.3) | 17.4(0.4) | -1.3(0.4) |

**References**


[1] V. Dohnal, D. Fenclova, P. Vrbka, *J Phys Chem Ref Data* **2006**, *35*, 1621-1651.
[2] D. Fenclova, V. Dohnal, P. Vrbka, V. Lastovka, *J Chem Eng Data* **2007**, *52*, 989-1002.
[3] S.J. Gill, B. Richey,G. Bishop, J. Wyman, *Biophysical Chemistry* **1985**, *21*,1-14.
[4] M. Heyden, J. Sun, S. Funkner, G. Mathias, H. Forbert, M. Havenith and D. Marx, *PNAS* **2010** 107, 12068-12074.
[5] https://www.schrodinger.com/watermap
[6] Dor Ben Amotz, Annu. Rev. Phys. Chem. 2016.67:617-638